PHYSICAL REVIEW B **80**, 161411(R) (2009)

Optical absorption of diamond nanocrystals from *ab initio* density-functional calculations

Márton Vörös and Adam Gali

Department of Atomic Physics, Budapest University of Technology and Economics, Budafoki út 8, H-1111 Budapest, Hungary

(Received 11 August 2009; revised manuscript received 7 October 2009; published 23 October 2009)

Absorption spectrum of small nanodiamonds, i.e., diamondoids has been recently measured exhibiting features that are not understood. Previous calculations, even beyond standard density-functional theory (DFT), failed to obtain the experimental optical gaps (E_g) of diamondoids. We show that all-electron time-dependent DFT (TD-DFT) calculations including hybrid functional in the TD-DFT kernel are able to provide quantitatively accurate results. Our calculations demonstrate that Rydberg transitions are characteristic even for relatively large nanodiamonds resulting in low E_g. The nonmonotonic size dependence of E_g is explained by symmetry considerations.

DOI: 10.1103/PhysRevB.80.161411 PACS number(s): 78.67.Bf, 71.15.Qe, 73.22.−f

The optical gap of semiconductor nanoparticles (NP) can be tuned by reducing their size that is called the quantum confinement (QC) effect.[1] This is now a major focus of nanoscale research in the applications of biomarkers, photovoltaics, and photocatalysis; therefore, understanding the optical properties of small semiconductor NPs is of high interest. Due to computational limitations, accurate *ab initio* methods for calculating optical response of NPs are restricted to single, perfect, and isolated structures[2–5] with relatively small particle size which cannot be directly compared to experimental data taken usually from larger NPs with unknown surface structure and various size distributions.

Recently, ultrasmall diamond nanoparticles (DNP), also called diamondoids, containing 10–26 carbon atoms have been isolated and purified from petroleum.[6] The resulted DNPs were selected by different size and shape via high performance chromatography.[6] The optical spectrum of the 99% purified DNPs have been very recently detected by ultraviolet absorption spectroscopy at room temperature and above.[7] The obtained optical spectrum of DNPs measured by Landt *et al.*[7] is rather surprising because, (i) contrary to the indications of previous experimental[8–10] and theoretical studies,[11,12] the optical gaps do not show a clear monotonic decrease as the function of the size of DNPs, (ii) the optical gaps are relatively close to the indirect band gap of bulk diamond, and (iii) none of recent theoretical studies could predict quantitatively the optical gaps of nanodiamonds, e.g., Diffusion Monte Carlo (DMC) calculations overshot the gap by ≈ 1 eV.[12]

The DNPs fabricated by Landt *et al.*[7] have a fundamental importance: (i) their chemical structure is *exactly known*, (ii) they build perfect bulklike structures, and (iii) their surface is perfectly passivated by hydrogen atoms. The absorption spectrum of the selected DNPs was recorded in the gas phase that makes possible the *direct* comparison of the measured and calculated spectrum. Experiments on these diamondoids have revealed a special role of DNPs within the group IV family of nanocrystals.[8] In addition, the nanodiamond materials have increasing significance in the nanoscale materials science and technology.[13–16] The present discrepancy between theory and experiment may stem the successful application of small diamond nanoparticles.

In this Rapid Communication, we calculate the absorption spectrum of diamondoids (Fig. 1) by time-dependent density-functional theory (TD-DFT) using all-electron high quality basis set. We apply PBE0[17] hybrid functional in the TD-DFT kernel. We show that the calculated and measured optical gaps are within 0.15 eV. The nonmonotonic size dependence of the optical gaps is explained by the symmetry of DNPs. In addition, we are able to identify the Rydberg excitations in their absorption spectrum that explains the relatively small optical gap of DNPs.

We studied all the diamondoids that were measured in the experiment.[7] The structures are shown in Fig. 1 where we label their name and symmetry. The smallest diamond cage is called adamantane, which has 10(16) carbon(hydrogen) atoms. By adding more carbon atoms to this cage, one can build larger nanodiamonds with different shapes and symmetry where all the surface carbon atoms bind to only one or two hydrogen atoms. We define the effective diameter (d) of diamondoids as the largest distance between any two carbon atoms in DNPs.

The geometry of the diamondoids was optimized by the supercell plane-wave PWSCF code[18] using ultrasoft pseudopotentials[19] and PBE functional[20] at DFT level. We used 35 Ry for the wave function cutoff and 280 Ry for the charge density cutoff. We applied >10 Å vacuum between the periodic images of the structures that provides charge density and geometry without spurious interaction between them. We allowed the relaxation of all the atoms until the forces were below the given threshold of 0.001 Ry/Bohr. We used these optimized geometries in further calculations. The absorption spectrum of DNPs was calculated with the cluster code TURBOMOLE[21] at TD-DFT level with hybrid functional

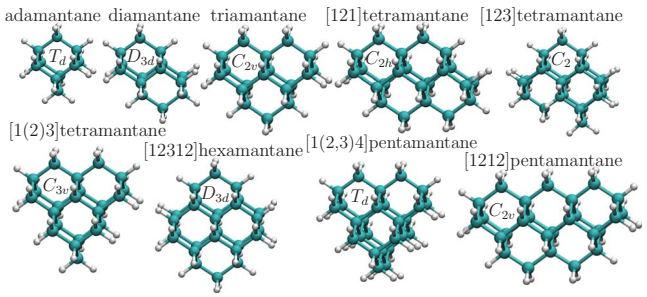

FIG. 1. (Color online) Ball and stick geometries of the studied diamondoids: their name and point group symmetry.

TABLE I. The atomic structure of the studied DNPs and their calculated gaps. First, second, third, and fourth columns: name of DNPs, chemical structure, symmetry, and its diameter (d) in nm. Fifth, sixth, seventh, eighth, and ninth columns: calculated PBE, TDPBE, PBE0, TDPBE0, and DMC gaps (Ref. 12) in eV, respectively. Exp1 shows the experimental gap with $C=0.0005$ (Ref. 7) while Exp2 with $C=0.001$ (see details in text). H→L(n): the contribution of HOMO→LUMO+n transition to the onset of absorption in %.

Name	DNP	Sym.	d	PBE	TDPBE	PBE0	TDPBE0	DMC	Exp1	Exp2	H→L(n)
Adamantane	$C_{10}H_{16}$	T_d	0.36	5.73	5.79	7.53	6.66	7.61(2)	6.49	6.55	98(0)
Diamantane	$C_{14}H_{20}$	D_{3d}	0.46	5.41	5.87	7.15	6.75	7.32(3)	6.40	6.47	98(1)
Triamantane	$C_{18}H_{24}$	C_{2v}	0.56	5.17	5.21	6.89	6.12		6.06	6.10	98(0)
[123]Tetramantane	$C_{22}H_{28}$	C_2	0.64	5.04		6.74	6.01		5.95	5.98	98(0)
[121]Tetramantane	$C_{22}H_{28}$	C_{2h}	0.69	5.04		6.71	6.25		6.10	6.15	98(2)
[1(2)3]Tetramantane	$C_{22}H_{28}$	C_{3v}	0.56	5.09		6.78	6.04		5.94	5.96	97(0)
[1(2,3)4]Pentamantane	$C_{26}H_{32}$	T_d	0.56	5.03		6.70	5.99	7.04(6)	5.81	5.85	97(0)
[1212]Pentamantane	$C_{26}H_{32}$	C_{2v}	0.80	4.91		6.57	5.86		5.85	5.90	97(0)
[12312]Hexamantane	$C_{26}H_{30}$	D_{3d}	0.64	4.87		6.54	6.12		5.88	5.91	97(1)

PBE0 in the kernel.[22] The PBE0 hybrid functional uses 25% mixing of Hartree-Fock exchange into the PBE functional where the mixing parameter was derived from perturbation theory.[17] We applied frequency domain linear response TD-DFT method to calculate the lowest lying dipole allowed singlet transitions. We note that Ciofini and Adamo showed on small molecules consisting of 3–5 atoms that due to the well-behaving asymptotic behavior of the PBE0 functional one can achieve quantitatively good results for the absorption spectrum even in the presence of low lying Rydberg states when PBE0 functional in the TD-DFT kernel is applied.[23] We emphasize that no spurious interaction between the DNPs occurs in the cluster code during the calculation of the absorption spectrum that could be present in a supercell approach. TURBOMOLE utilizes localized basis functions. We found in agreement with Ref. 12 that very high level of basis set was needed for convergent calculations. We applied an all-electron aug-cc-pVTZ basis set.[24]

Next, we discuss the experimental absorption spectrum of DNPs. The threshold of absorption of the measured spectra (E_{gap}) was determined by a simple integration criterion, $\int_0^{E_{\mathrm{gap}}}\mathrm{Abs}(E)dE=C\int_0^{E_{\max}}\mathrm{Abs}(E)dE$, where "Abs" is the intensity of the absorption and C is a small positive number. According to Ref. 7, C is set to 0.0005. The error bar of this procedure for the optical gap was estimated to be 0.03 eV.[7] The obtained numbers are listed in column "Exp1" of Table I. By close inspection of the experimental spectra revealed us that they are relatively noisy showing wiggles that might be due to the not 100% purity of the samples and temperature effects. In the column "Exp2"of Table I we show the derived optical gaps with $C=0.001$. By comparing columns Exp1 and Exp2, it is apparent that all the optical gap values remain approximately in the estimated error bar except for diamantane: the gap was shifted upward by ~0.07 eV. In any case, the optical gaps are very close to the band gap of bulk diamond, 5.45 eV. The average diameter of the DNPs is very small and much larger optical gaps (with several eV) are expected from simple QC effect.[1] In addition, no clear trend is visible between the diameter and optical gaps of the DNPs. In Table I, we compare the experimental data with recent available DMC results.[12] DMC overshoots the optical gap by ≈1 eV. We show our TD-DFT results for the optical gaps in column TDPBE0 of Table I. We obtained discrete transitions in our calculations. In order to simulate the finite lifetime of the excited states we applied a Lorentzian broadening of 0.002 Ry on each peak. The overall agreement with the experiment is very good. The absolute mean error is ≈0.15/0.11 eV when comparing to Exp1/Exp2 values. The largest deviation comes from the difference between the measured and calculated optical gap of diamantane (≈0.3 eV). Our result indicates that the absorption spectrum of diamantane may be remeasured possibly with better purification of the sample and/or at lower temperature. We note here that the temperature effects further complicate the direct comparison of the calculated and measured spectrum. The strong C-C (~0.2 eV) and C-H (~0.4 eV) vibrations at elevated temperatures "smear" the experimental spectra, particularly at high energies where the excited states are close to each other in energy. At low energy region, characteristic vibration bands in the spectrum appear as blue shift next to the peak of pure electronic transitions.[25] We treated the structures statically, thus smearing effects due to vibrations were not taken into account in our calculations. Since vibrations broaden the peaks, the calculated optical gaps would be even closer to the experimental values. All in all, our calculated optical gaps follow closely the experimental values and show no clear trend of QC effect. The optical gaps are indeed relatively close to the band gap of bulk diamond. We note here that TD-DFT optical gaps with traditional LDA (Ref. 26) or PBE functionals (Table I) yield too low values compared to the experiments.

Our calculations make possible to reveal the nature of the optical gap of DNPs. In a crude approximation the optical gap is the energy difference between the Kohn-Sham DFT levels of lowest unoccupied molecular orbital (LUMO) and highest occupied molecular orbital (HOMO). In earlier calculations,[7,12] the delocalization of LUMO has been shown and it was referred to as "surfacelike state." In addition, it has been found[8,12] that LUMO energies show no QC effect at all while HOMO energies do show. We also found that LUMO energies are within 0.1 eV for all DNPs while the energy of HOMO increases by about 1.0 eV going from ada-

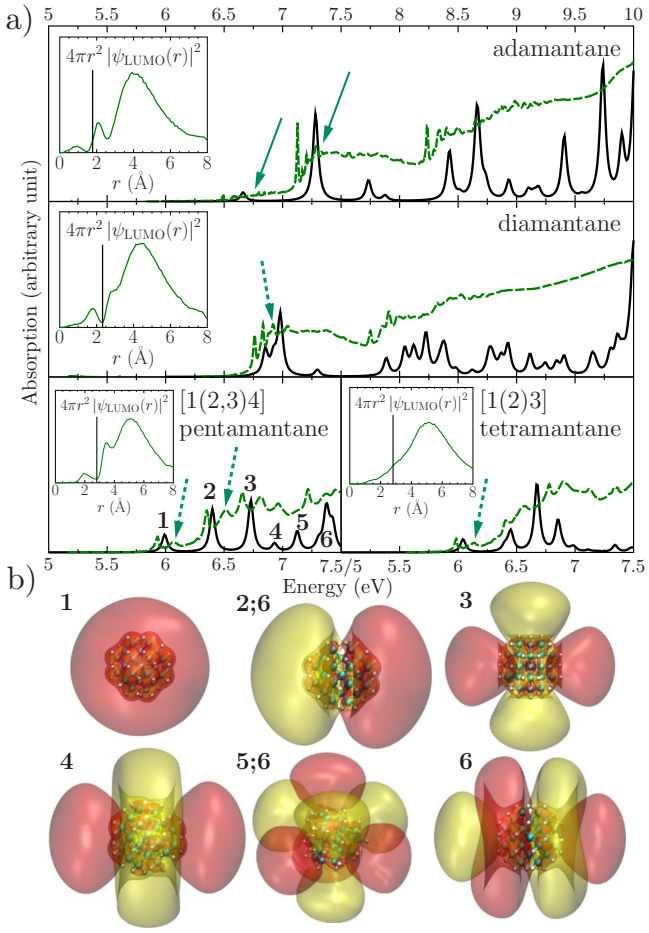

FIG. 2. (Color online) (a) Calculated and experimental absorption spectrum for selected diamondoids. Green (dashed) line shows the experimental spectrum while black (continuous) line is the calculated spectrum. Arrows: see text. Inset: radial distribution function of LUMO; vertical line: radius of DNP (b) States associated with Rydberg-like excitations in [1(2,3)4]pentamantane are illustrated and indicated with numbers in the spectrum. Red (dark gray) and yellow (light gray) lobes show the selected positive and negative isovalues of the corresponding PBE0 unoccupied states. Large (small) spheres indicate C(H) atoms.

mantane to pentamantane.[27] We demonstrate that LUMO is not a surface state but a 3*s*-like Rydberg state. The Bohr radius of this Rydberg state is about twice of the radius of the corresponding DNPs explaining the almost size independent LUMO energies. 3*s* Rydberg state character of LUMO is particularly evident for T_d symmetry structures [see the insets in Figs. 2(a) and 2(b)1] and less visible for DNPs with lower symmetry. Obviously, the *s*-like Rydberg states are distorted at larger extent for DNPs with lower symmetry than with T_d symmetry. The QC effect of HOMO energies with the fixed energy position of LUMO would still indicate QC effect of the gap in this crude approximation (see the PBE gaps in Table I), thus the nonmonotonic size dependence of the measured optical gap is not explained by the nature of LUMO.

The symmetry influences not only the shape of LUMO. The selection rules govern which transitions are allowed in the absorption. Now, we restrict our analysis only for the

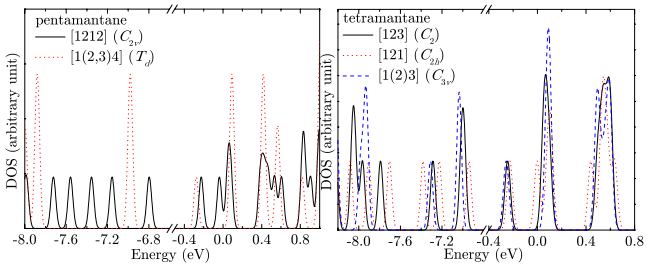

FIG. 3. (Color online) Density of states close to HOMO and LUMO for DNPs with same number of atoms but different point group symmetries as indicated. Note the broken axis in midgap.

pure electronic transitions. Then, the optical gap may be approximated as the first *allowed* dipole transition between the Kohn-Sham DFT states. We realized that the symmetry of the measured DNPs widely scatters that strongly influences the transition probability. In the case of low symmetries (C_2, C_{2v}, C_{2h}) the single particle states can mix to each other forming wider spectrum and there will be only few or no such pairs of states where the transitions are dipole-forbidden. Figure 3 shows this trend clearly for the occupied states near HOMO: the higher the symmetry the more "peaky" is the density of states. The trend is not so visible for the unoccupied states near LUMO consisting of delocalized states. We note here that the excitation energy was defined in the DMC calculation[12] as the energy difference of the excited and ground states where the excited state was constructed by changing the occupation number of HOMO and LUMO orbitals of the ground state to zero and one, respectively. In the case of diamantane, this may be not a correct method since the LUMO state does not contribute to the first transition. The role of symmetry has been recently recognized in Ref. 7 parallel to our study based on DFT calculations. However, DFT is a ground state theory, thus principally, it cannot certainly provide the true single particle states contributing to the optical gap of DNPs. Time-dependent DFT methods can provide reliable excitation spectrum. By analyzing our TDPBE0 results we found that the optical gaps are primarily (over 97%) originated from the single particle transition from HOMO to LUMO or to LUMO+1 or to LUMO+2 depending on the selection rule. For instance, tetramantane with C_{2h} symmetry has the first dipole active transition between HOMO and LUMO+2 while between HOMO and LUMO for C_{3v} and C_2 symmetry structures. This will raise the optical gap of C_{2h} configuration by about 0.2 eV with respect to that of the other two structures. This is the main reason why no clear QC effect occurs for these small DNPs.

Next, we plot the calculated and measured absorption spectra of DNPs in Fig. 2. Apart from a small energy shift of about 0.15 eV, our calculated excitation spectra follow closely the experimental spectra except for the vibration bands (marked by solid arrows for adamantane known experimentally,[25] and by dashed arrows suggested by us in analog with adamantane, shown in Fig. 2), particularly at low energy region.

The nature of the peaks in the absorption spectra of DNPs is generally not understood. Raymonda demonstrated for the

smallest DNP, adamantane, that the second sharp peak is a Rydberg excitation.[25] Based on the fit of the selected sharp peaks to the Rydberg equation, Raymonda claimed that the second sharp peak is a $3p$ excitation while the first sharp peak might be a $3s$ excitation.[25] Raymonda also suggested that the first transitions should be the excitations from the nondegenerate a_1 state in order to explain that the intensity of $3s$ peak is smaller than that of $3p$ peak, or if the transition occurs from the degenerate t_2 state than the first sharp peak might be a $4p$ Rydberg excitation.[25] Landt *et al.* claimed that the sharp resonances characteristic for Rydberg excitations vanished for larger DNPs.[7] We demonstrate on the spectrum of [1(2,3)4]pentamantane with T_d symmetry in Fig. 2 that the first optical transition is a typical Rydberg excitation to a $3s$-like state despite the t_2 character of HOMO, and the higher energy sharp peaks also show the character of Rydberg excitation with higher order of angular momenta. The first peak is associated with a HOMO→LUMO transition where the HOMO is a triply degenerate t_2 state strongly localized within the DNP (not depicted) showing no atomic orbital character at all while LUMO is a $3s$ Rydberg state [Fig. 2(b)1]. The second sharp peak is a three-times degenerate $3p$ Rydberg transition that transform as t_2 in T_d symmetry [Fig. 2(b)2]. We note that this picture holds for adamantane as well. Despite, HOMO transforms as t_2 the ratio between the calculated oscillator strength of HOMO→$3s$ and HOMO→$3p$ transitions is about 3(10) for pentamantane(adamantane). Both $t_2 \rightarrow a_1(3s)$ and $t_2 \rightarrow t_2(3p)$ transitions are allowed but the latter has higher joint density of states that will lead to larger intensity in the absorption for the $3p$ Rydberg excitation. We were able to identify the responsible unoccupied states participating in "1–6" transitions as shown in Fig. 2(b). Above the s and p states we could identify d-like [Figs. 2(b)3 and 2(b)4] and f-like [Figs. 2(b)5 and 2(b)6] states. The d and f-like states split due to T_d symmetry. Some f states perturbed considerably by the antibonding bulklike orbitals. We emphasize that the Rydberg series in the absorption spectrum are not typical for such large semiconductor nanoparticles. For instance, silicon nanocrystallites with similar size and shape have been recently investigated by TD-DFT method but no delocalized state has been reported.[5] Our calculations revealed that even the largest diamondoids measured recently by Landt *et al.* have Rydberg excitation in the spectrum[7] despite the fact that they have not been unambiguously recognized but only for adamantane. While we show our results for [1(2,3)4]pentamantane in detail, we emphasize here that the nature of the first peak is common for all the DNPs: it is a $3s$-like Rydberg excitation except for diamantane, [121]tetramantane, and [12312]hexamantane, where $3s$-like Rydberg excitations are dipole-forbidden; therefore, $3p$-like Rydberg transitions occur. We note that the delocalization of the spherical functionlike empty states makes the convergent calculation within supercell approach very challenging and indicate that the typical vacuum size applied for the ground state calculations, ~ 1 nm, is not sufficient for the excited states of isolated nanodiamonds.

A.G. acknowledges the support from Hungarian OTKA under Grant No. K-67886, the NIIF Supercomputer center under Grant No. 1090 and the János Bolyai program of the Hungarian Academy of Sciences.

[1] L. E. Brus, J. Chem. Phys. **80**, 4403 (1984).
[2] M. Rohlfing and S. G. Louie, Phys. Rev. Lett. **80**, 3320 (1998).
[3] I. Vasiliev, S. Öğüt, and J. R. Chelikowsky, Phys. Rev. Lett. **86**, 1813 (2001).
[4] L. X. Benedict, A. Puzder, A. J. Williamson, J. C. Grossman, G. Galli, J. E. Klepeis, J. Y. Raty, and O. Pankratov, Phys. Rev. B **68**, 085310 (2003).
[5] L. E. Ramos, J. Paier, G. Kresse, and F. Bechstedt, Phys. Rev. B **78**, 195423 (2008).
[6] J. E. Dahl, S. G. Liu, and R. M. K. Carlson, Science **299**, 96 (2003).
[7] L. Landt, K. Klunder, J. E. Dahl, R. M. K. Carlson, T. Moller, and C. Bostedt, Phys. Rev. Lett. **103**, 047402 (2009).
[8] T. M. Willey, C. Bostedt, T. van Buuren, J. E. Dahl, S. G. Liu, R. M. K. Carlson, L. J. Terminello, and T. Moller, Phys. Rev. Lett. **95**, 113401 (2005).
[9] T. M. Willey, C. Bostedt, T. van Buuren, J. E. Dahl, S. G. Liu, R. M. K. Carlson, R. W. Meulenberg, E. J. Nelson, and L. J. Terminello, Phys. Rev. B **74**, 205432 (2006).
[10] K. Lenzke *et al.*, J. Chem. Phys. **127**, 084320 (2007).
[11] A. J. Lu, B. C. Pan, and J. G. Han, Phys. Rev. B **72**, 035447 (2005).
[12] N. D. Drummond, A. J. Williamson, R. J. Needs, and G. Galli, Phys. Rev. Lett. **95**, 096801 (2005).
[13] A. P. Marchand, Science **299**, 52 (2003).
[14] W. L. Yang *et al.*, Science **316**, 1460 (2007).
[15] Y. Wang *et al.*, Nature Mater. **7**, 38 (2008).
[16] M. Romalis, Nature (London) **455**, 606 (2008).
[17] J. P. Perdew, M. Ernzerhof, and K. Burke, J. Chem. Phys. **105**, 9982 (1996).
[18] P. Giannozzi *et al.*, J. Phys.: Condens. Matter **21**, 395502 (2009).
[19] D. Vanderbilt, Phys. Rev. B **41**, 7892 (1990).
[20] J. P. Perdew, K. Burke, and M. Ernzerhof, Phys. Rev. Lett. **77**, 3865 (1996).
[21] R. Ahlrichs *et al.*, Chem. Phys. Lett. **162**, 165 (1989).
[22] R. Bauernschmitt and R. Ahlrichs, Chem. Phys. Lett. **256**, 454 (1996).
[23] I. Ciofini and C. Adamo, J. Phys. Chem. A **111**, 5549 (2007).
[24] K. L. Schuchardt *et al.*, J. Chem. Inf. Model. **47**, 1045 (2007).
[25] J. W. Raymonda, J. Chem. Phys. **56**, 3912 (1972).
[26] J. Raty and G. Galli, J. Electroanal. Chem. **584**, 9 (2005).
[27] We used the $1s$ Kohn-Sham levels of C atoms as reference energy.